Quasistatic rheology of foams: I. Low strain response

Alexandre Kabla, Georges Debregeas

Quasistatic rheology of foams I. Low strain response

By ALEXANDRE KABLA[1] AND GEORGES DEBREGEAS[2]

[1] Division of Engineering and Applied Sciences, Harvard University, Pierce Hall, 29 Oxford Street, Cambridge, Massachusetts 02138, USA

[2]Laboratoire de Physique Statistique, Ecole Normale Supérieure, CNRS - UMR 8550, 24 Rue Lhomond, 75231 Paris Cedex 05,FRANCE

A quasistatic simulation is used to study the mechanical response of a disordered, bidimensional aqueous foam submitted to an oscillating shear strain. The application of shear appears to progressively extend the elastic domain, i.e. the strain range within which no plastic process occurs. It is associated with the development of an irreversible normal stress difference, and a decrease in the shear modulus, which both are signatures of the appearance of anisotropy in the film network. Beyond this mechanical measurement, the evolution of the structural properties of the foam is investigated. We focus in particular on the structural energy E_0 defined as the minimum line-length energy under zero shear stress. For strain amplitude less than ~ 0.5, this quantity is found to decay with the number of applied cycles as a result of the curing of topological defects. However, for higher strain amplitude, plastic events appear to increase the structural disorder and tend to gather near the shearing walls. This process is a precursor of the shear-banding transition observed in fully developed flows, which will be studied in the companion paper.

The rheology of soft glasses has been the subject of an increasing number of studies in the last two decades. This class of systems includes macroscopically divided materials such as foams, concentrated emulsions, colloidal suspension or dense granular packings, but also multicontact frictional joints (Baumberger (2005)) or dense assemblies of vertices in class II superconductors (Fisher (1991)). As in a molecular glass below T_g, the thermal energy in these systems is low compared to the energy barriers for structural relaxation. In the absence of external stress, the system is thus permanently trapped in a metastable configuration. This results in the existence of a finite yield stress below which the material responds elastically. When a larger stress is imposed, it triggers a series of local depinning processes which release the applied stress, yielding a macroscopic flow.

This particular mode of stress relaxation has numbers of rheological consequence. First, it allows for the existence of a quasistatic regime of flow when the strain rate is lower than the depinning rate (Khan (1988), Rouyer (2005)). In this regime, the stress/strain curve shows an initial quasi-linear regime. The stress then reaches a maximum before decaying asymptotically to a constant lower value. This strain weakening behaviour is referred to as localization in the literature since it is usually interpreted as a signature of the appearance of spatially heterogeneous flow. Beyond this transition, the stress signal, measured on small systems, is intermittent: it exhibits a series of linear increases interrupted by rapid drops associated with the successive depinning events. Another characteristic feature of these systems is the so-called strain-induced aging process: the dynamical properties continuously vary with the application of a moderate shear (Viasnoff (2002)).

This indicates that even a low strain can trigger a few depinning events which modify the mesoscopic structure, that controls, in turn, the macroscopic mechanical response (Bureau (2002)).

Numerous models have been proposed to interpret this set of observations. Some of them, inspired or derived from glass theory, introduce a parameter which plays the role of a temperature in order to recover a thermodynamical description (Sollich (1997), Liu (1998)). This so-called "effective temperature" is generally described as a function of the flow field itself. It results in a shear dependent fluidity which has been directly postulated in Derec (2001). Although such models may reproduce the phenomenology of the rheology, they lack a convincing description of the local mechanisms which would justify the proposed form for the effective temperature and its coupling with the flow. An alternative approach, inspired by the pioneering work of Bulatov and Argon (Bulatov (1994)), has been proposed by Falk and Langer (Falk (1998)). They observe in a numerical simulation of amorphous and athermal systems of interacting spheres, that plasticity is associated with discrete and local rearrangements involving a few particles. This observation is at the base of the STZ (Shear Transformation Zone) model, which links a microscopic description of the plastic event to the macroscopic rheology. All these models require to properly relate the local strain rate with the stress tensor and local structural properties and to characterize spatial interactions between plastic events. Therefore, a system where one can follow both the structure and the rheology is needed to further test and refine these different approaches.

Aqueous foams constitute a convenient model system to study plasticity in solid materials. It allows one to directly monitor the deformation of a crystalline or disordered structure at the level of its individual components, as was first recognized by Bragg who used crystalline bubbles rafts as a tool for understanding the dynamics of dislocations in metals (Bragg (1947)). Foam coarsening - the bubble disproportionation induced by gas diffusion between neighbouring bubbles - can be viewed as a process analogous to grain growths in metals (Weaire (1984)). More recently, disordered foams have proven to be a rich heuristic system for the study of glassy rheology. Along this line, we have recently developed a quasi-2D foam system which consists of a monolayer of bubbles confined between two horizontal plates (Debrégeas (2001)). This system exhibits shear-banding under slow deformation in cylindrical Couette geometry. Using a numerical foam simulation, a similar flow behaviour was evidenced in plane parallel shear (Kabla (2003)).

In these two articles, we attempt to understand the connection between the mechanical properties and the structural state of a foam under two types of solicitation. In the present article, we study numerically the response of a foam to an oscillating strain, using the code developed in Kabla (2003). In the second companion article, we investigate fully developed shear flow, experimentally and numerically.

1. Numerical model

The wetness of a bidimensional foam is characterized by the area fraction of gas Φ. For $\Phi > 0.86$, the foam exhibits a finite yield stress. Here we focus on the limit of dry foams $\Phi \sim 1$. In this regime, the foam is composed of polyhedral bubbles separated by thin liquid films (Weaire (1999)). Three films intersect in regions called vertices, where most of the water is present (see figure 1(a)). Plasticity in 2D dry foams arises through rapid local neighbour-switching events called $T1$ processes, as described on figure 1(a) and (b).

Several models have been developed to describe the behaviour of 2D dry foams under finite shear rate (Q-Potts models (Jiang (1999)), Vertex model (Okuzono (1993), Oku-

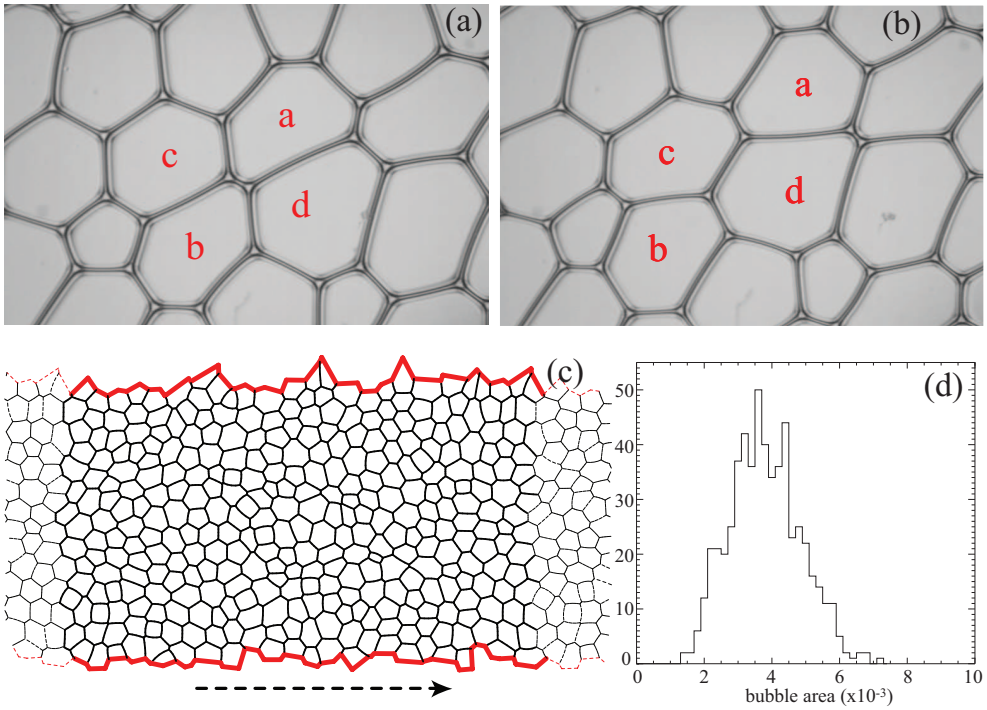

FIGURE 1. (a) and (b): a T1 plastic event observed in a confined 2D foam (Debregeas (2001)). This elementary plastic process involves a neighbours exchange between 4 bubbles indicated by the letters in the two successive pictures. (c) The numerical 2D foam used in the present study. Shearing is obtained by incrementally moving the lower (rigid) boundary as indicated by the arrow. The foam is periodic along the shear direction. (d) Area distribution of the bubbles.

zono (1995))). To capture static or zero shear rate properties, a precise modelling of the fast energy dissipation during the T1 process is unnecessary. The quasistatic algorithms (Weaire (1983), Herdtle (1992), Weaire (1999)), based on the time-scale separation between the short duration of the plastic events τ_{T1} and the long characteristic time of shearing, provide a realistic description of the dynamics.

When the time-scale associated with the imposed strain is large compared to the rearrangement time, the foam is at any time mechanically equilibrated (except during the rapid rearrangements). The foam structure minimizes the *static* free energy of the foam: for incompressible bubbles†, this energy is proportional to the total film length. Vertices have a typical size d_v related to the amount of water in the foam (figure 1). When the distance between two vertices is close to d_v, the foam becomes unstable and bubbles rearrange through the T1 (figure 1(a-b)). The quasistatic shear simulation developed here is based on these arguments, and involves a loop over three main steps: (1) one first computes the geometrical foam structure for the current bubbles arrangement (the neighbouring relation between bubbles): the total film length is minimized under prescribed boundary conditions (described later) and keeping constant each bubble volume. (2) The stability of the resulting structure with respect to topological rearrangements is then tested: when a film length falls below a threshold value (chosen to correspond to

† The state equation of the gas is *a priori* necessary. However, for millimetric bubbles and typical surface tensions, the resulting relative changes in volume are negligible and the bubbles can be assumed incompressible.

a gas fraction $\Phi = 0.99$) a topological change occurs. The minimal line-length structure is then recalculated. Steps (1) and (2) are repeated until the structure is stable with regards to plastic events. (3) A small increment of deformation is then applied, and the whole process of relaxation is started again.

The initial foam is created from the Voronoi tessellation of a disordered set of points (Weaire (1999)), obtained by superimposing a Gaussian random displacement to an hexagonal lattice. The noise amplitude is used to tune the distribution of the resulting bubble areas. In this paper, the dimensions of the foams are $L_x \times L_y = 1.5 \times 1$, the system is periodic along the x direction and is confined in the y direction by two rigid and rough walls (see figure 1(c)). Around 400 bubbles are packed between the two parallel walls. Their area distribution is presented in figure 1(d). In our unit system, the mean area and the standard deviation are respectively around $4 \cdot 10^{-3}$ and $1 \cdot 10^{-3}$.

The energy minimization consists in the determination of the vertices positions and films curvatures which correspond to a minimum of the total line length. To reach this configuration, we use Surface Evolver (SE) (Brakke (1992)), a minimization software which has proved to be reliable for the computation of foam structures (Reinelt (2000), Kraynik (2003)). The gradient descent algorithm of SE rapidly ensures a locally equilibrated structure by computing the forces on each vertex and projecting the resulting trajectories along constraints (constant volume here). However, for extended networks, a dramatically large number of iterations is needed to relax the soft modes of deformations associated with large length-scale deformation fields. To bypass this limitation, the minimization process is separated into two distinct steps: (1) the foam structure is first reduced to a set of vertices connected by straight lines. The energy landscape associated with the structure is probed by imposing large length-scale incompressible deformation fields, such as elementary shear or local rotation. When one of these strain fields decreases the total line-length energy, the associated displacement of the vertices is implemented. (2) When this minimization process has converged, the structure is progressively refined by adding degrees of freedom along the edges (up to eight points per edge). All the different physical quantities studied in this paper are measured on this final structure. This method proves to significantly enhance the convergence of the minimization, and allows to study minute global deformation observed in real experiments (Debrégeas (2001)). The details, tests and justification of this procedure can be found in Kabla (Thesis).

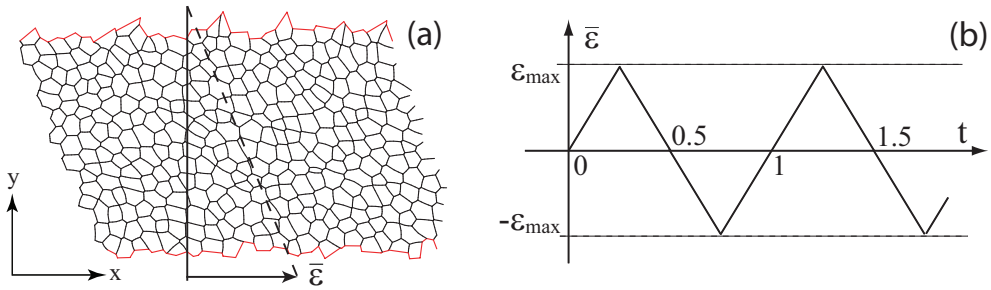

FIGURE 2. (a) A foam sample (16x24 bubbles) submitted to an imposed strain of amplitude $\bar{\epsilon}$. (b) The oscillating strain sequence imposed to the foam in a typical experiment: t is the number of cycles and ϵ_{max} is the maximum strain amplitude.

Shearing is imposed by progressively moving the lower wall from left to right, by small shear strain increments of 0.5%. As expected in quasistatic regime, moving the lower wall

is strictly equivalent to moving the upper wall in the opposite direction. From this point forward, lengths are scaled by the width L_y of the shearing gap, so that the displacement d of the lower wall is also the mean strain $\overline{\varepsilon} = d/L_y$. It should be noted that $\overline{\varepsilon}$ is the only control parameter for this study.

2. Quasistatic rheology

The foam is submitted to an average strain oscillating between two symmetrical limits ϵ_{max} and $-\epsilon_{max}$. As physical time is irrelevant in the quasistatic regime, affine displacements are used and the evolutions of different structural and mechanical parameters are monitored as a function of the fractional number of applied cycles t (figure 2). †

2.1. *Stress-strain relationship*

The coarse-grained shear stress over any sub-region S of the sample can be extracted from the structure of the foam by using the following equation (Kraynik (2003)):

$$\sigma_{xy}(\mathcal{D}) = \frac{\gamma}{A(\mathcal{D})} \cdot \sum_{\text{films i}} \frac{l_{i,x} \cdot l_{i,y}}{l_i} \tag{2.1}$$

The sum is performed over all the films laying within the sub-region $\mathcal{D}$ of area $A(\mathcal{D})$. l_i is the length of the film, $l_{i,x}$ and $l_{i,y}$ are the projected length over the horizontal and vertical axis respectively. From this point forward, the line tension γ of the liquid film is set at 1.

By performing this calculation over the entire sample, the evolution of the total shear stress $\overline{\sigma_{xy}}$ exerted by the moving walls can be monitored. This quantity is shown in Figure 3(a) as a function of the number of cycles t for different values of ϵ_{max} (dotted lines indicate the imposed strain). These graphs illustrate the elasto-plastic behaviour of foams under quasistatic shear: under low strain, the stress-strain relationship is linear. For imposed strain $\epsilon_{max} \geq 0.5$, the stress reaches a yield value σ_Y. However, careful examination of the graphs reveals the occurrence of yielding events for stress values lower than the yield stress, especially during the first elastic charge (inset in Figure 3(a)).

2.2. *Transient, limit cycles and hysteresis*

Figure 3 shows the evolution of the shear stress with respect to the imposed strain, for different strain amplitudes. Consistently with the experimental measurements of Rouyer *et al.* (Rouyer (2003)), it reveals that the mechanical response of the foam is modified by the first cycles of deformation (shear aging). After a few oscillations, a limit cycle is reached beyond which no apparent evolution of those properties can be detected. For a maximum strain $\overline{\epsilon}_{max} < 0.5$, no more T1 event occurs after one or two cycles. For $\overline{\epsilon}_{max} \geq 0.5$, some irreversibility persists (figure 3(b)) and the associated dissipated energy can be measured by computing the area of the hysteresis loops in the limit cycle (relation 2.2):

$$\Delta E_\infty = A \oint_{\text{limit cycle}} \sigma_{xy}(\epsilon) \mathrm{d}\epsilon \tag{2.2}$$

where $A = L_x L_y$ denotes the total foam area. Figure 3(c) shows the evolution of this quantity for various strain amplitudes. ΔE_∞ is strictly zero for $\epsilon_{max} < 0.5$ then

† Videos of these simulations are available online (`http://tel.ccsd.cnrs.fr/docs/00/04/56/98/HTML/CisAlternFlash.htm`).

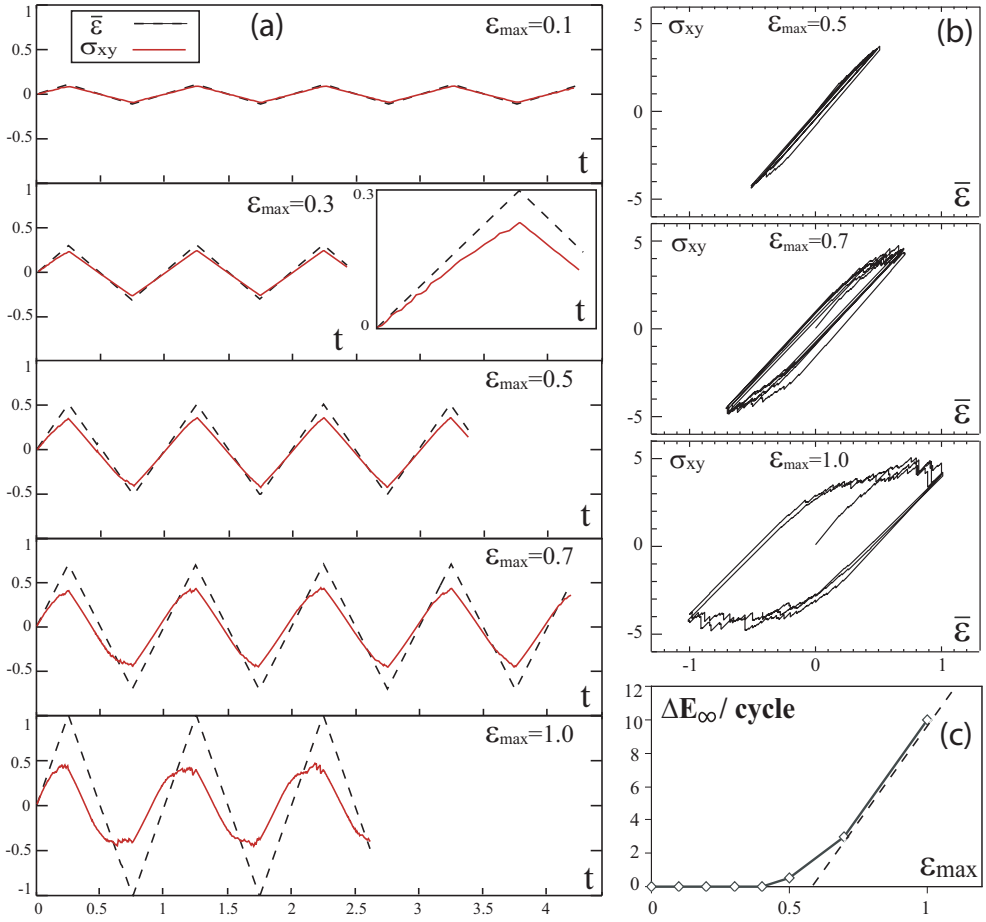

FIGURE 3. (a) imposed strain (dotted lines) and shear stress (solid lines) as a function of t for different amplitudes strain amplitudes ϵ_{max} (a magnification of 0.1 has been imposed to the stress measurements for clarity). The inset is a zoom of the first charge for $\epsilon_{max} = 0.3$. (b) Hysteresis cycles for different amplitudes. When $\epsilon_m ax < 0.5$, the behaviour becomes purely elastic after a transient of one or two cycles. (c) Energy dissipated per cycle in permanent regime as a function of the shear strain amplitude.

monotonously increases with ϵ_{max}. In a rough approximation, ΔE_∞ can be described in that regime as a linear function of the imposed strain:

$$\Delta E_\infty = 4\ A\ \sigma_Y\ (\epsilon_{max} - \bar{\epsilon}_Y) \tag{2.3}$$

This allows one to identify the yield stress σ_Y and the yield strain ϵ_Y as the maximum stress and strain that the foam can sustain elastically. It should be noted however that these quantities are not intrinsic to the material: they may depend on the specific structure (the particular arrangement of the bubbles) of the foam, as well as its dimension.

2.3. *Development of normal stress difference*

Development of normal stress difference is a characteristic feature of foams rheology (Reinelt (1996)) which is also observed in other complex systems such as polymers (Barnes (1989)). In order to investigate this process, we focus on the regime of large applied strain ($\epsilon_{max} = 1$). Figure 4 shows the first normal stress difference $\sigma_{xx} - \sigma_{yy}$ as a

function of the number of cycles t and of the shear stress σ_{xy}. These graphs illustrate the strong coupling between these two quantities: the normal stress difference can be empirically described as a quadratic function of σ_{xy} with an offset $\Delta\sigma_{n,0}$ being a function of the number of cycles t:

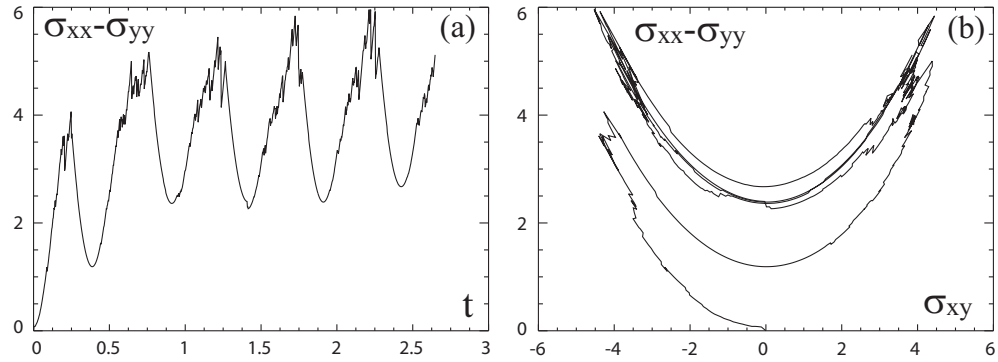

FIGURE 4. First normal stress difference as a function of (a) the number of shear cycles and (b) the shear stress. The maximum strain amplitude is $\epsilon_{max} = 1$.

$$\sigma_{xx} - \sigma_{yy} = \Delta\sigma_{n,0}(t) + \beta \cdot \sigma_{xy}^2 \tag{2.4}$$

The quadratic part results from the elastic deformation of the film network, as will be detailed in the next section. This behaviour has been evidenced in previous numerical studies (Reinelt (1996), Reinelt (2000)), but the measurements were performed on crystalline foams which do not show irreversible structural evolution under shear. In contrast, our disordered foam undergoes irreversible structural changes during the transient regime, which result in a permanently imprinted anisotropy of the material. To quantify this process, the normal stress difference under zero shear stress $\Delta\sigma_{n,0}$ is evaluated by extrapolating the parabolic sections of the graphs of Figure 4. As shown in figure 5, this quantity, plotted as a function of the number of applied strain cycles, exhibits (sample dependent) fluctuations about a slow global increase.

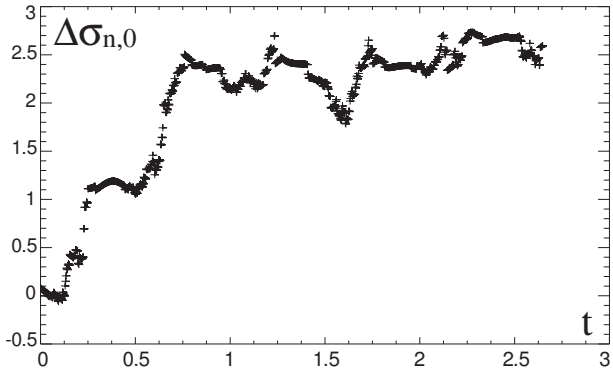

FIGURE 5. Normal stress difference under zero shear stress $\Delta\sigma_{n,0}$ as a function of the number of cycles t (maximum strain amplitude $\epsilon_{max} = 1$).

2.4. *Energetic approach*

In order to investigate the modification of the structural properties of the system under shear, we consider the evolution of the foam free energy (total line-length) with the imposed strain $\bar{\epsilon}$ (figure 6). For the lowest strain amplitude $\epsilon_{max} = 0.1$, no rearrangement occurs during the first cycle of charge and discharge. The strain is reversible and the stress is a quadratic function of the strain. The following charge in the opposite direction generates one T1 event, which induce a transition to a different energy basin.

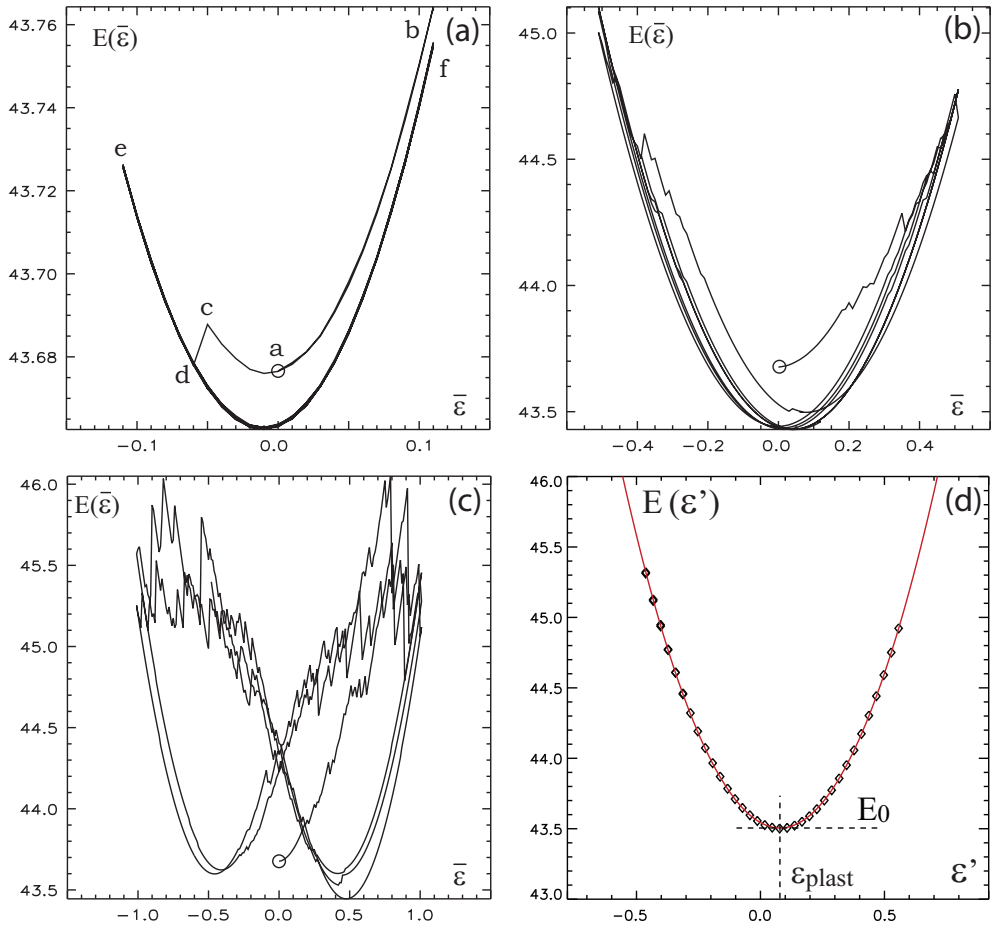

FIGURE 6. (a,b,c)Free energy of the foam as a function of the imposed strain, for three different amplitudes ϵ_{max} =0.1, 0.5 and 1.0. The circles indicate the initial state, and the number of applied cycles is 3. The chronological trajectory in (a) is [a,b,a,c,d,e,d,f,d,e,d,f,...] (d) Quadratic elastic basin associated with a given structure (see text). Symbols are numerical measurements, and the curve corresponds to the best parabolic fit.

The evolution of the system under shear can thus be seen as a series of transitions, induced by discrete plastic events, in a multistable potential landscape. Each configuration is associated with an elastic basin, which properties can be accessed by a quadratic extrapolation of the local energy versus deformation curve. The extrapolation must be performed in the elastic domain of response, in which no rearrangement takes place, and thus becomes increasingly inaccurate when the applied strain approaches the yield strain limit (figure 6(b) and 6(c)). To bypass this limitation, a specific numerical proce-

dure is implemented: for every structure successively reached, a complete shear cycle of amplitude 0.5 is performed in which topological changes are forbidden. This numerical procedure allows one to produce an extended elastic basin, as shown in figure 6(d), on which a quadratic fit can be performed:

$$E(\varepsilon') = E_0 + \frac{A\mu}{2}\,(\varepsilon' - \varepsilon_{plast})^2 \tag{2.5}$$

where A the foam area, μ is the shear modulus and E_0 is the minimal value of the energy reached under zero shear stress. These two latter quantities are specific to the structure and do not depend on the elastically stored shear deformation. It should be noted that E_0 cannot be extracted from mechanical measurements which only depend on the derivative of the potential. Henceforth, E_0 will be referred to as the structural energy of the foam. The quantity ϵ_{plast} corresponds to the applied strain (associated with a particular position of the lower wall) for which the foam energy is minimum and the shear stress is 0.

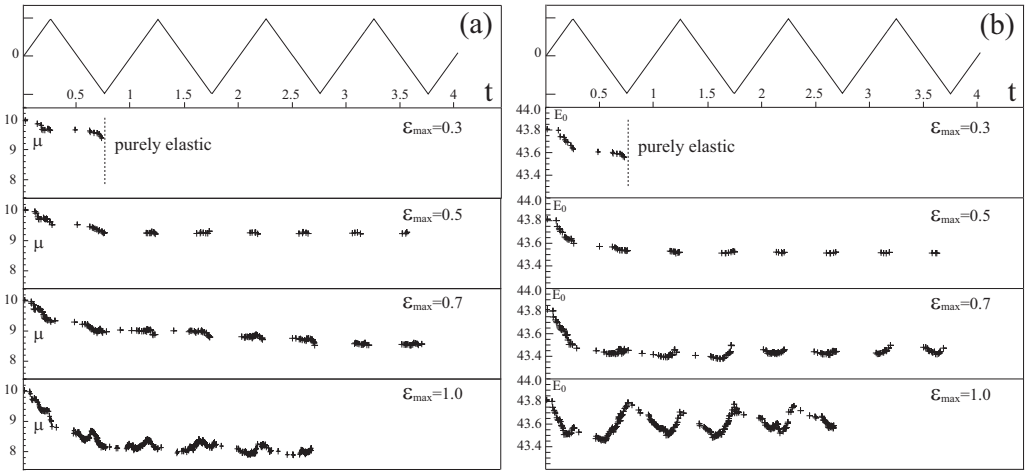

FIGURE 7. Evolution of (a) the shear modulus μ and of (b) the structural energy E_0 with the number of applied cycles t for different strain amplitudes (the top graphs show the associated imposed strain sequence). These quantities are evaluated after each T1 event and plotted at the instant of the rearrangement. For the lowest strain amplitude, no rearrangement occurs after the first cycle. Since the calculation time becomes extremely long, the experiment was run for 3 cycles instead of 4 for the largest strain amplitude.

Figure 7 shows the evolution of the shear modulus μ and of the structural energy E_0 as the foam undergoes successive strain oscillations. A systematic decrease of μ is observed with the number of cycles, this effect being stronger for increasing strain amplitude. The same behaviour is observed for E_0 which indicates the existence of a strain-induced structural relaxation process. For large shear amplitude however ($\varepsilon_{max} > 0.7$), the value of the structural energy exhibits oscillations: its value reaches a maximum whenever the absolute value of the applied strain is maximum. This behaviour is associated with the development of spatial inhomogeneities of the T1 events positions as will be shown later in the article.

3. Interpretation

The structural evolution of the foam under moderate shearing ($\varepsilon_{max} < 0.7$) is associated with (i) the appearance of normal stress difference, (ii) a structural energy relaxation, (iii) a decrease of the shear modulus. These evolutions result from the strain-induced topological rearrangements that irreversibly modify the foam structure. In this section, we attempt to account for these observations by first examining the effect of the film network anisotropy on both the normal stress difference and the shear modulus, using a simplified foam model. We then focus on the evolution of topological disorder to interpret the decrease in the structural energy.

3.1. *Shear modulus and normal stresses*

As first recognized by Princen (Princen (1983)), the main characteristics of foam elasticity can be understood by considering the film elongation induced by the deformation of a regular network of liquid films. Following Alexander's foam model (Alexander (1998)), we consider a square network of films with dimension $L_x \times L_y$, and surface tension γ. R denotes the distance between adjacent films in the original (undeformed) structure (figure 8(a)). This simplified model ignores disorder as well as the Plateau's rule that imposes films to meet at an angle of 120 degree. When the network is strained along the horizontal x-direction, the length of the horizontal films remains unchanged, whereas the length of the vertical films varies with the shear strain ϵ_{xy} by a quantity:

$$\delta l(x) = L_y \cdot \sqrt{1+\epsilon_{xy}^2} - L_y \tag{3.1}$$

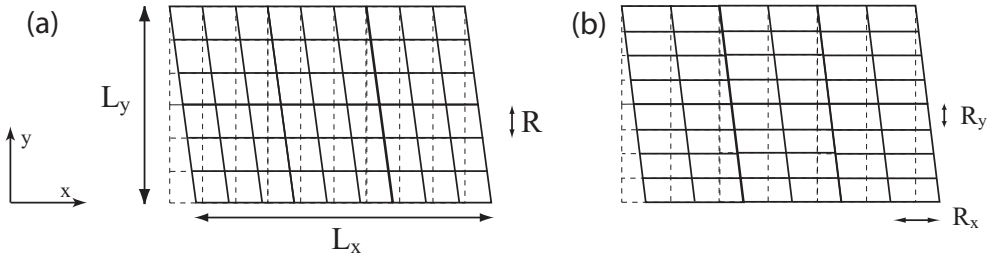

FIGURE 8. Simplified foam models: (a) isotropic: a square films network is sheared along the x-axis (the dotted grid represents the unsheared configuration), (b) anisotropic: the foam consists of rectangular cells which deform into parallelograms as the system is sheared .

Assuming that each film acts on the structure with a force of intensity γ, simple geometry allows one to write the different components of the stress tensor to second order in the applied deformation ϵ_{xy}:

$$\sigma_{xy} = \mu_0 \cdot \epsilon_{xy} \tag{3.2}$$

$$\sigma_{xx} = \frac{\gamma}{R} \cdot \left(1+\epsilon_{xy}^2\right) = \mu_0 \cdot \left(1+\epsilon_{xy}^2\right) \tag{3.3}$$

$$\sigma_{yy} = \frac{\gamma}{R} \cdot \left(1-\frac{1}{2}\,\epsilon_{xy}^2\right) = \mu_0 \cdot \left(1-\frac{1}{2}\,\epsilon_{xy}^2\right) \tag{3.4}$$

where $\mu_0 = \frac{\gamma}{R}$ is the shear modulus†. The relationship between the shear stress and the normal stress difference immediately follows:

† A better estimate is obtained with an hexagonal network that takes into account the local equilibrium rule of the liquid films (Princen (1983))

$$\sigma_{xx} - \sigma_{yy} = \frac{3}{2}\frac{\gamma}{R} \cdot \epsilon_{xy}^2 = \frac{3}{2}\frac{R}{\gamma} \cdot \sigma_{xy}^2 \tag{3.5}$$

This rough model provides a quadratic relationship between shear stress and normal stress difference, as observed numerically. It should be noticed that a similar relationship is observed in polymers (Barnes (1989)) though the underlying mechanisms differ: in polymer solutions, shearing induces a deformation of the entangled chain network but the average orientation results from a competition between the imposed shear and the thermal relaxation of the polymer chains. Thus, the shear stress and normal stresses are controlled by the shear rate and not by the applied strain, as in the present situation.

$A = L_x \cdot L_y$ being the area of the foam, the total film-length or free energy of the system can also be written to second order in ϵ_{xy} as:

$$E(\epsilon_{xy}) \quad = \quad E_0 + \frac{1}{2} \cdot A \cdot \frac{\gamma}{R} \cdot \epsilon_{xy}^2 \tag{3.6}$$

$$\text{with } E_0 = \frac{L_x}{R} \cdot \gamma L_y + \frac{L_y}{R} \cdot \gamma L_x = \frac{2\gamma A}{R} \tag{3.7}$$

We observed in the preceding section the appearance of a finite normal stress difference under zero shear stress. This indicates that an oscillating strain induces a relative increase of the average density of films in the shear direction in comparison to the normal direction. In order to illustrate this effect, we introduce anisotropy in the previous model (Figure 8(b)) by considering a film network composed of parallelograms of size $R_x \times R_y$. The equivalent cell size is defined as $R = \sqrt{R_x \times R_y}$ and the structure anisotropy is characterized by two parameters:

$$\left\{ \begin{array}{lcl} \varepsilon_{xx} & = & R_x/R - 1 \\ \varepsilon_{yy} & = & R_y/R - 1 \end{array} \right. \tag{3.8}$$

Using an approach similar to the one used for the square lattice, the line-length energy now reads:

$$E(\varepsilon_{xy}) = E_0 + \frac{1}{2} \cdot A \cdot \frac{\gamma}{R} \cdot (1 - \varepsilon_{xx}) \cdot \epsilon_{xy}^2 \tag{3.9}$$

$$\text{with: } E_0 = \frac{2\gamma A}{R} \cdot \left(1 + \frac{1}{2}\varepsilon_{xx}^2 + \frac{1}{2}\varepsilon_{yy}^2\right) \tag{3.10}$$

The shear modulus thus writes:

$$\mu = \frac{1}{2A} \cdot \frac{\partial E}{\partial \epsilon_{xy}} = \frac{\gamma}{R} \cdot (1 - \varepsilon_{xx}) \tag{3.11}$$

The previous relations show that the anisotropy affects both the structural energy E_0 and the shear modulus. This simple model provides a prediction for the normal stress components as a function of the shear strain ϵ_{xy} and the anisotropy parameters ε_{xx} and ε_{xx}:

$$\sigma_{xx} = \frac{\gamma}{R} \cdot (1 - \varepsilon_{yy}) + \frac{\gamma}{R} \cdot (1 - \varepsilon_{xx}) \cdot \epsilon_{xy}^2 \tag{3.12}$$

$$\sigma_{yy} = \frac{\gamma}{R} \cdot (1 - \varepsilon_{xx}) - \frac{\gamma}{2R} \cdot (1 - \varepsilon_{xx}) \cdot \epsilon_{xy}^2 \tag{3.13}$$

To first order in ε_{xx}, the volume conservation ($R_x R_y = R^2$) imposes that $\varepsilon_{xx} + \varepsilon_{yy} = 0$, so that the normal stress difference under zero shear stress reads:

$$\sigma_{xx} - \sigma_{yy} = \underbrace{\frac{\gamma}{R} \cdot (2\varepsilon_{xx})}_{\Delta\sigma_{n,0}} + \frac{3}{2}\frac{\gamma}{R} \cdot (1 - \varepsilon_{xx}) \cdot \epsilon_{xy}^2 \tag{3.14}$$

By confronting this expression to the relation (3.11), one can derive a relationship between the normal stress difference under zero shear stress $\Delta\sigma_{n,0}$ and the shear modulus:

$$\mu = \mu_0 - \frac{1}{2}\Delta\sigma_{n,0} \tag{3.15}$$

where $\mu_0 = \frac{\gamma}{R}$ is the shear modulus of the equivalent isotropic foam.

This relation suggests to test the correlation between these two quantities measured in the numerical simulation. The expected proportionality is observed in spite of the fluctuations of these two parameters, as evidenced in figure 9. It should be noted however that the ratio $(\mu_0 - \mu)/\Delta\sigma_{n,0}$ is of the order of 0.8 in the numerical system instead of the expected 0.5 predicted by this model. This discrepancy can be accounted for by the simplicity of the model, which does not take into account neither the Plateau's rule nor the polydispersity of the foam. Nevertheless, it illustrates the fact that both quantities reflect the distribution of the films orientation with regards to the shearing direction. The strain-induced T1 processes tend to orientate the films in the direction of the shear thus driving the structure into an anisotropic state.

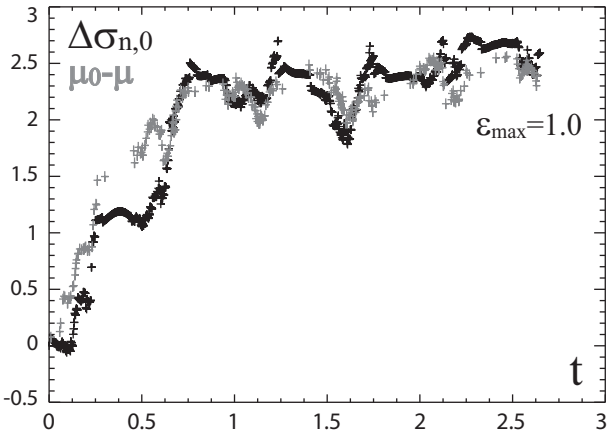

FIGURE 9. Normal stress difference under zero stress $\Delta\sigma_{n,0}$ (black) and variation of the shear modulus $\mu_0 - \mu$ (gray) as a function of the number of cycles t, extracted from the numerical simulation with a strain amplitude $\epsilon_{max} = 1$. The shear modulus variations have been multiplied by 1.25 to underline the similar evolution of both quantities.

3.2. *Relaxation of the disorder and transition to the plastic flow*

The anisotropic model presented above yields an expression of E_0 as a function of the anisotropy parameters (relation 3.10). Based on this expression, one would expect E_0 to increase with the imposed maximum strain, in contradiction with our observations. This model however ignores the foam disorder, and the possible evolution of this property with shearing, which one expects to modify E_0.

One standard way to evaluate topological disorder in dry foams consists in measuring

the second momentum μ_2 of the distribution $P(n)$ of the number of films per bubble (Weaire (1999)). In 2D dry foams, the average number of films per bubble is exactly 6, which yields the following expression for μ_2:

$$\mu_2 = \sum_n (n-6)^2 \cdot P(n) \tag{3.16}$$

In agreement with previous experimental (Abd el Kader (1999)) and numerical (Kraynik (2003)) studies, moderate shearing is observed to produce a partial relaxation of the topological disorder (figure 10). By curing topological defects originally present in the foam, the initial shearing extends the elastic domain. This shear-strengthening process has its counterpart in other systems such as dense colloidal glasses or friction joints (Viasnoff (2002), Bureau (2002), Baumberger (2005)). Although the decrease of E_0 under low strain can be accounted for by this topological relaxation, the oscillations of E_0 at larger deformation still remain unexplained. Neither the anisotropy (measured by the normal stresses difference at zero shear stress) nor the topological disorder (measured by μ_2) exhibit a similar behaviour.

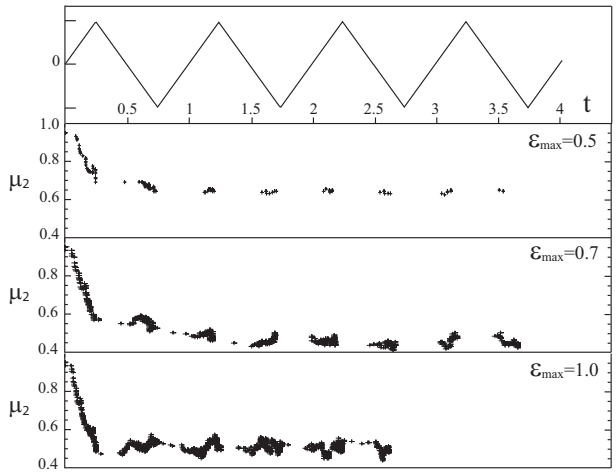

FIGURE 10. Evolution of the topological disorder. The second momentum μ_2 of the distribution of the number of films per bubble is plotted as a function of the number of applied cycle t for different strain amplitudes ϵ_{max}. The top graph shows the associated imposed strain sequence.

To understand this process, one needs to look into more details at the effect of T1 events on the energy basin of the foam. When a rearrangement T1 occurs during the shearing, a certain amount of energy δE is relaxed (figure 6). δE is found to be systematically of order $-\gamma D$, where D is the mean bubble diameter. This energy release may be decomposed into two terms, as sketched in figure 11:

$$\delta E = \delta E_0 - A\ \sigma_{xy}\ \delta\epsilon_{plast} \tag{3.17}$$

The first term is associated with a relaxation of the structural energy E_0. The second one corresponds to a partial relaxation of the applied shear stress σ_{xy}, which induces a lateral shift in the position of the minimum of the energy basin. The relative value of the structural and shear stress relaxation strongly depends on the system preparation. Figures 6 and 7(b) show that, under low deformation, T1 events mainly relax the structure. In contrast, under high deformation, the main effect of the rearrangements is a relaxation

of the applied shear stress. When the shear stress becomes high, δE_0 (equation 3.17) can be positive, leading to the increase of E_0 observed in figure figure 7(b): the stress release occurs at the expense of the structure relaxation. The oscillations of the structural energy may therefore be understood as a series of shear stress relaxations (which increase the structural heterogeneities) and disorder relaxations when the shear stress is reversed.

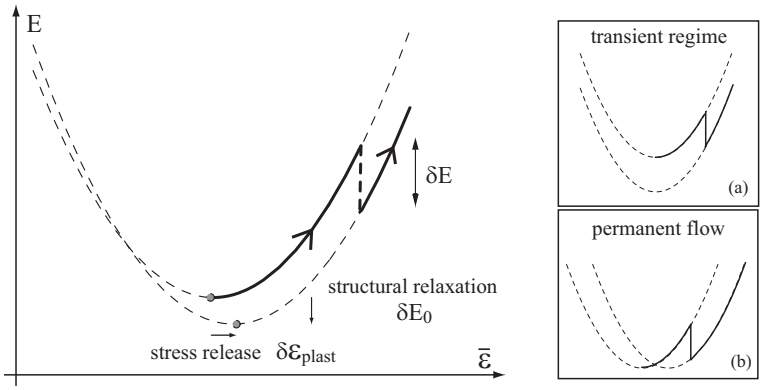

FIGURE 11. Shift of the elastic basin following a T1 event. Two main mechanisms can be distinguished: (a) relaxation of the structural disorder (mostly during transient regime), and (b) relaxation of the imposed shear stress.

The transition to plastic flow can also be studied by looking at the spatial distribution of the rearrangements during shearing (Figure 12). For low strain amplitude $\epsilon_{max} \leq 0.5$, T1 events are uniformly distributed inside the foam. For higher amplitude in contrast, they occur preferentially in the vicinity of the walls. These observations are consistent with the appearance of a shear-band observed under continuous slow shear in a similar geometry (Kabla (2003)). Because the random initial foam is homogeneously disordered, the first structural relaxation (the transient regime) produces rearrangements uniformly distributed inside the sample. Beyond the transient, the rheological response becomes sensitive to the constraint imposed by the rigid walls, which then induces the observed inhomogeneities in the spatial distribution of rearrangements.

Discussion and Conclusion

The response of a 2D foam to an oscillating quasistatic shear exhibits a transient regime, which corresponds to the first few cycles, during which different mechanical properties evolve with time. The elastic domain (the strain range within which no plastic process occurs) is enlarged and the shear modulus decreases as the topological disorder is reduced. The shear-induced plastic events tend to orientate the film preferentially along the shear direction, which results in a decrease of the shear modulus and the development of normal stress difference. For a moderate amplitude of strain ($\epsilon_{max} \leq 0.5$) the plastic events are homogeneously distributed. Beyond this limit, they tend to preferentially occur along the rigid walls and this transition is associated with a sudden increase of the free energy of the system. This corresponds to the entrance into the large strain regime which will be studied in the companion paper.

In the permanent regime, the foam exhibits a highly non-linear rheological response: it behaves elastically up to a yield stress (or strain), beyond which it flows under a well defined shear stress (Khan (1988)). In standard rheological measurements, this non-

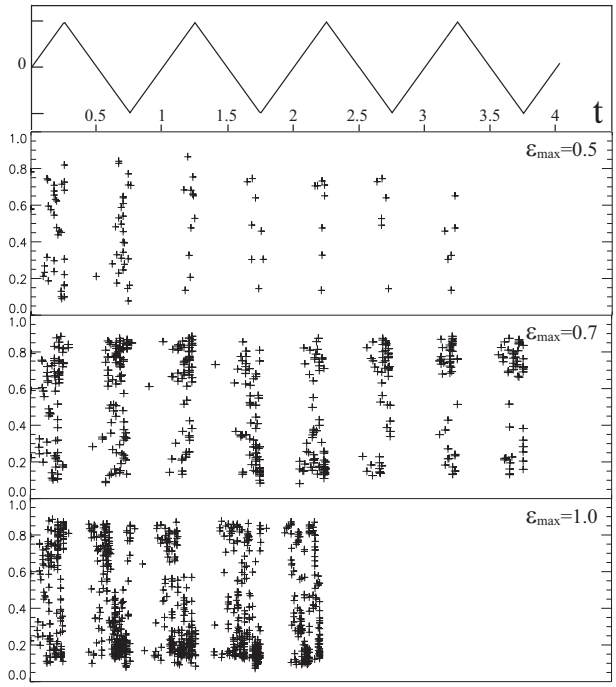

FIGURE 12. Positions of the T1 rearrangements across the gap during the shearing, for different amplitude ε_{max}. For each T1 event, occurring at the instant t, a cross is placed which ordinate corresponds to its distance to the lower wall.

linearity is expected to show up as a dependence of the complex shear modulus $G = G' + iG''$ with the strain amplitude at vanishingly small shear rates, as recently evidenced by Rouyer *et al.* (Rouyer (2005) and references therein). Considering that the energy dissipated per cycle can be written as $\Delta E \approx G''\varepsilon_{max}^2$, one expects the loss modulus to depend on the strain amplitude as:

$$G'' \propto \sigma_Y \frac{\varepsilon_{max} - \varepsilon_Y}{\varepsilon_{max}^2} \tag{3.1}$$

for strain amplitudes larger than the yield strain ε_Y; G'' should be null otherwise. This relation appears to be in good agreement with the recent measurements of Rouyer et al. (Rouyer (2005)) for imposed shear strain larger than the yield strain. The behaviour at low deformation is however more puzzling: although a linear regime seems to exist for low enough strain amplitude, G'' is found to exhibit non-zero limit as the shear amplitude is decreased. This behaviour cannot be explained in the scope of the present model, but it might indicate that the threshold for plasticity strongly depends on the dimensionality and volume of the foam sample (Kraynik (2003)). This discrepancy could also results from the existence of processes associated with long time-scales, such as coarsening or drainage (Hohler (2005) and references therein), which are not included in this numerical model.

REFERENCES

ABD EL KADER, A. & EARNSHAW, J. C. 1999 Shear-Induced Changes in Two-Dimensional Foam *Phys. Rev. Lett.* **82**, 2610–2613.

Alexander, S. 1998 Amorphous solids: their structure, lattice dynamics and elasticity *Physics Reports* **296**, 65–236.

Barnes, H.A., Hutton, J.F. & Walters, K., An Introduction to Rheology, 2003, vol. 3, Rheology series, Elsevier.

Baumberger, T. & Caroli, C. 2005 Solid Friction from stick-slip to pinning and aging *cond-mat/0506657*

Bragg, L. & Nye, J. F., 1947, A dynamical model of a crystal structure, *Proc. R. Soc. London A* **190**, 474–482.

Brakke, K. 1992 The Surface Evolver *Experimental Mathematics* **1**, 141–165.

Bulatov, V.V. & Argon A.S. 1994 A stochastic model for continuum elasto-plsatic behavior: I. Numerical approach and strain localization *Modelling Simul. Mater. Sci. Eng.* **2**, 167–184.

Bulatov, V.V. & Argon A.S. 1994 A stochastic model for continuum elasto-plsatic behavior: II. A study of the glass transition and structural relaxation *Modelling Simul. Mater. Sci. Eng.* **2**, 185–202.

Bulatov, V.V. & Argon A.S. 1994 A stochastic model for continuum elasto-plsatic behavior: III. Plasticity in ordered versus disordered solids *Modelling Simul. Mater. Sci. Eng.* **2**, 203–222.

Bureau, L., Baumberger, T. & Caroli, C. 2002 Rheological aging and rejuvenation in solid friction contacts *Eur. Phys. J. E* **8**, 331-337.

Debrégeas, G., Tabuteau, H. & di Meglio, J.-M. 2001 Deformation and flow of a Two-Dimensional Foam under Continuous Shear *Phys. Rev. Lett.* **87**, 178305.

Derec, C., Ajdari, A. & Lequeux, F. 2001 Rheology and aging: A simple approach, *Eur. Phys. J. E* **4**, 355–361.

Falk, M.L. & Langer, J.S. 1998 Dynamics of viscoplastic deformation in amorphous solids *Phys. Rev. E* **57**, 7192.

Fisher, D. S., Fisher, M. P. A. & Huse, D. A. 1991 Thermal fluctuations, quenched disorder, phase transitions, and transport in type-II superconductors *Phys. Rev. B* **43**, 130–159.

Herdtle, T. & Aref, H. 1992 Numerical experiments on two-dimensional foam, Journal of Fluid Mechanics **241**, 233.

Hohler, R. & Cohen-Addad, S. 2005 Rheology of liquid foam, J. Phys.: Condensed Matter **17**, R1041–R1069.

Jiang, Y., Swart, P.J., Saxena, A., Asipauskas, M. & Glazier, J.A. 1999 Hysteresis and avalanches in two-dimensional foam rheology simulations, Phys. Rev. E **59**, 5819.

Kabla, A. & Debrégeas, G. 2003 Local stress relaxation and shear-banding in a dry foam under shear, *Phys. Rev. Lett.* **90**, 258303.

Kabla, A. 2003 PhD Thesis, University Paris 7. Available online at `http://tel.ccsd.cnrs.fr/`

Khan, S. A., Schnepper, C. A. & Armstrong, R. C. 1988 Foam rheology: III Measurement of shear flow properties, *Journal of Rheology* **32**, 69–92.

Kraynik, A.M., Reinelt, D.A. & van Swol, F. 2003, Structure of random monodisperse foam, *Phys. Rev. E* **67**, 031403.

Liu, A. & Nagel, S.R. 1998 Nonlinear dynamics Jamming is not just cool any more *Nature* **396**, 21–22.

Okuzono, T., Kawasaki, K. & Nagai, T. 1993 Rheology of random foams, *Journal of Rheology* **37**, 571.

Okuzono, T. & Kawasaki, K. 1995 Intermittent flow behavior of random foams: A computer experiment on foam rheology *Phys. Rev. E* **51**, 1246–1253.

Princen, H.M. 1983 Rheology of foams and highly concentrated emulsions : I. Elastic properties and yield stress of a cylindrical model system *Journal of Colloid and Interface Science* **91**, 160–175.

Reinelt, D.A. & Kraynik, A.M. 1996 Simple shearing flow of a dry Kelvin soap foam, *J. Fluid Mech.* **311**, 327.

Reinelt, D.A. & Kraynik, A.M. 2000 Simple shearing flow of dry soap foams with tetrahedrally close-packed structure, *Journal of Rheology* **44**, 453.

Rouyer, F., Cohen-Addad, S., Vignes-Adler, M. & Holler, R. 2003 Dynamics of yielding observed in a three-dimensiomal aqueous dry foam, *Phys. Rev. E* **67**, 021405.

Rouyer, F., Cohen-Addad, S. & Holler R. 2005 Is the yield stress of aqueous foam a well-defined quantity?, *Colloids and Surfaces A* **263**, 111–116.

Sollich, P., Lequeux, F., Hébraud, P. & Cates, M.E. 1997 Rheology of soft glassy materials, *Phys. Rev. Lett.* **78**, 2020.

Viasnoff, V. & Lequeux, F. 2002 Rejuvenation and Overaging in a Colloidal Glass under Shear, *Phys. Rev. Lett.* **89**, 065701.

Weaire, D. & Kermode, J.P. 1983 Computer simulation of a two-dimensional soap froth I. Method and motivation, *Philosophical Magazine B* **48**, 245–259.

Weaire, D. & Kermode, J.P. 1984 Computer simulation of a two-dimensional soap froth II. Analysis of results, *Philosophical Magazine B* **50**, 379–395.

Weaire, D. & Hutzler, S. 1999 The Physics of Foams, Clarendon Press, Oxford.